Applied Geochemistry 106 (2019) 17–25

Contents lists available at ScienceDirect

Applied Geochemistry

journal homepage: www.elsevier.com/locate/apgeochem

# Occurrence, source, and partition of PAHs, PCBs, and OCPs in the multiphase system of an urban lake, Shanghai

Jing Yang[a], Abdul Qadeer[a], Min Liu[a,b,*], Jun-Min Zhu[a], Yan-Ping Huang[a], Wei-Ning Du[a], Xin-Yi Wei[a]

[a] Key Laboratory of Geographic Information Science of the Ministry of Education, School of Geographic Sciences, East China Normal University, 500 Dongchuan Road, Shanghai, 200241, China
[b] Institute of Eco-Chongming (IEC), 3663 N. Zhongshan Road, Shanghai, 200062, China

ARTICLE INFO

Editorial handling by Dr K Hanna

*Keywords:*
POPs
Distribution
Source analysis
Partition
Health risk
Dianshan lake

ABSTRACT

Dianshan Lake (DSL) as an important water source protection area in Shanghai is facing serious water quality deterioration. A detailed investigation of persistent organic pollutants (POPs) including polycyclic aromatic hydrocarbons (PAHs), polychlorinated biphenyls (PCBs), and organochlorine pesticides (OCPs) in the multiphase system of DSL is very important for understanding their occurrence, sources, partition, and health risks. Total 11 sampling sites were selected including 3 inflowing rivers, 6 lake body sites, and 2 outflowing rivers. Total OCPs ($\Sigma_{20}$OCPs) showed the highest concentration in water dissolved phase with a range of 47.8–143 ng/L. Total PAHs ($\Sigma_{16}$PAHs) were the dominant compounds for suspended particle matter (SPM) and sediment phase, with a range of 2805–4130 and 206–4262 ng/g, respectively. The nonparametric test revealed the significantly higher concentrations of $\Sigma_{16}$PAHs in sediment, $\Sigma_{18}$PCBs in SPM, and $\Sigma_{20}$OCPs in dissolved water from inflowing rivers than lake body ($p < 0.05$), indicating the strong effect of riverine pollution input. The different seasonal distribution between $\Sigma_{16}$PAHs with $\Sigma_{18}$PCBs/$\Sigma_{20}$OCPs in SPM phase of lake body was closely attributed to their source disparities and the changes of rainfall and hydrodynamic conditions. Homologue compositions and isomer ratios analysis showed in DSL watershed PAHs were mainly derived from pyrogenic sources, PCBs from the leakage of capacitor equipment, sewage drainage of industries, and exfoliation of ship paints, and DDT from historical and recent application. The bioaccumulations of POPs in six fish species (n = 20) of DSL had high detection frequencies and a descending concentration order: $\Sigma_{16}$PAHs (353 ± 106 ng/g) > $\Sigma_{20}$OCPs (67.4 ± 27.0 ng/g) > $\Sigma_{18}$PCBs (32.0 ± 13.7 ng/g), with obvious species-specific characteristics. The partitioning behaviors of PAH congeners in the water-SPM-sediment-fish system of DSL were greatly influenced by log$K_{ow}$ values. However, the feeding habits (e.g., sediment-feeding behavior) of fish species played a predominant role in the bioaccumulation of PCB and OCP congeners compared to two-phase partition. Health risk assessments of POPs in dissolved water and fish samples revealed that only $\Sigma_{16}$PAHs in dissolved phase have potential carcinogenic risk.

## 1. Introduction

Semi-volatile persistent organic pollutants (SPOPs) such as polycyclic aromatic hydrocarbons (PAHs), polychlorinated biphenyls (PCBs), and organochlorine pesticides (OCPs) have attracted worldwide attention due to their persistence, bioaccumulation, toxicity, long-range transportation, and health hazard on organisms (Bettinetti et al., 2016; Carlson and Swackhamer, 2006; Li et al., 2017). Various aquatic ecosystems as pivotal natural reservoirs have received abundant inputs of anthropogenic SPOPs via atmospheric deposition and surface runoff. Especially in highly urbanized and industrialized areas, the gradual deterioration of aquatic environment has been a focus problem, accompanied by high SPOP accumulations in aquatic ecosystem (Li et al., 2017; Liu et al., 2016; Qin et al., 2014). For example, Li et al. (2017) conducted a national investigation of SPOPs (PAHs, PCBs, and OCPs) in lake sediments of China, and found their descending contamination levels from the highly urbanized eastern plain plateau to the remote Mongolia-Xinjiang plateau. Some large urban lakes such as Taihu Lake and Chaohu Lake in Yangtze River Delta (YRD, the most developed urbanized areas) of East China have been comprehensively investigated

* Corresponding author. Key laboratory of Geographic Information Science of the Ministry of Education, School of Geographic Sciences, East China Normal University, 500 Dongchuan Road, Shanghai, 200241, China.
*E-mail address:* mliu@geo.ecnu.edu.cn (M. Liu).

https://doi.org/10.1016/j.apgeochem.2019.04.023
Received 21 January 2019; Received in revised form 26 April 2019; Accepted 30 April 2019
Available online 02 May 2019
0883-2927/ © 2019 Published by Elsevier Ltd.

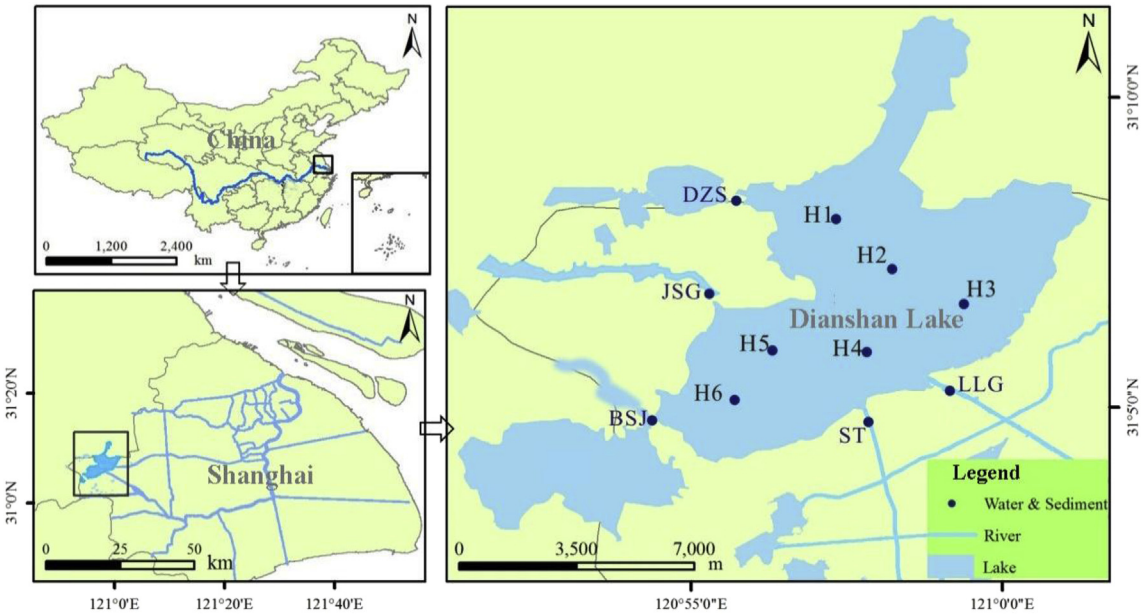


**Fig. 1.** Location of Dianshan Lake watershed and sampling sites of water and sediment.

for the occurrence, distribution and risk of SPOPs (Liu et al., 2017; Qin et al., 2014; Wang et al., 2018). However, a systematic investigation of SPOPs in some relatively small urban lakes of YRD region has been rarely documented.

Dianshan Lake (DSL, 120°52′-122°12′ E, 30°40′-31°53′ N) is the largest freshwater lake and one of the main drinking water resources in Shanghai (the hyper-urbanization city in YRD), with an area of 62 $km^2$ and average 2 m depth (Fig. 1). In the past two decades, the rapid urbanization development in YRD region have promoted DSL watershed to transform from a traditional agricultural area to be a flourishing area in economic growth and industrial development. In 2014, the proportions of four land use types (commercial, residential, industrial, and agricultural land) in the 3-km buffer around DSL were 16%, 57%, 21%, and 6%, respectively (Yang et al., 2019). However, rapid urbanization development and large-scale population growth have caused DSL to suffer from mixed contaminations from sewage drainage of industrial or residential activities, agricultural runoff, aquaculture, and vessel transportation, thereby aggravating its ecosystem degeneration. Unfortunately, a series of water treatment measures for DSL in recent years did not curb the trends of water quality deterioration. Therefore, considering the safety of the aquatic ecosystem, it is very urgent to take DSL as an example to comprehensively investigate the occurrence, sources, partition, and health risks of SPOPs in small urban lakes of YRD. The main objectives of this study were (i) to investigate the contamination levels and spatiotemporal distributions of three groups of SPOPs (PAHs, PCBs, and OCPs); (ii) to identify their possible sources by means of compositions and isomer ratios; (iii) to reveal their partitioning behaviors in the multiphase system; (iv) to evaluate their human health risks via oral exposure to water and fish resources of DSL.

## 2. Materials and methods

### 2.1. Sample collection

Total three inflowing rivers (DZS, JSG, and BSJ) and two outflowing rivers (ST and LLG) around DSL were selected. Further, six sites from lake body (H1–H6) were selected to collect overlying water and surface sediment samples in four seasons of 2016 (Fig. 1). Water samples (12 L) from each site were collected by organic glass hydrophore and stored in brown glass bottles. Surface sediment samples from each site were collected by using a stainless steel bottom sampler (XDB0201, New Landmark) and soon after collection samples were wrapped with aluminum foil and stored in sealed bags wrapped in aluminum foil. Six fish species (n = 20) including herbivore (*Ctenopharyngodon idellus*), carnivore (*Chanodichthys erythropterus* and *Erythroculter ilishaeformis*), and omnivore (*Carassius auratus*, *Pelteobagrus fulvidraco*, and *Cyprinus carpio*) were caught by casting a net into the lake handled by local fishermen in October 2016. All the samples were immediately transported on ice to labortory, and water samples were analyzed within 24 h soon after collection. The fish samples were dissected to obtain muscle tissue. All samples were kept at −20 °C until further analysis.

### 2.2. POPs and organic carbon analysis

Each water sample (4 L) was filtered by 0.45 μm glass microfiber filter (GF/F, Whatman) prebaked at 450 °C for 4 h to separate dissolved phase and suspended particle matter (SPM) phase. POPs in dissolved phase were spiked with 200 ng of terphenyl-$d_{14}$ (for PAHs) and 200 ng of 2,4,5,6-Tetrachloro-m-xylene (for PCBs/OCPs), respectively, and then extracted by using solid phase extraction (SPE) device with activated C18 cartridges and 5 mL/min water flow (Liu et al., 2016). Subsequently, PAHs, PCBs, and OCPs were eluted with 15 mL mixture of dichloromethane (DCM) and hexane (V:V, 3:7), 5 mL of hexane, and 10 mL mixture of DCM and hexane (V:V, 1:1), respectively. These eluents were further concentrated to 1 mL under high purity nitrogen and added 200 ng internal standards (naphthalene-$d_8$, acenaphthene-$d_{10}$, phenanthrene-$d_{10}$, chrysene-$d_{12}$, and perylene-$d_{12}$ for PAHs, o-Nitrobromobenzene and PCB209 for PCBs, and p,p'-DDE-$d_8$ and PCB209 for OCPs, respectively) before the instrument analysis.

All surface sediment, SPM, and fish samples were freeze-dried, ground, and sieved through a 0.15 mm mesh. Approximately 0.1 g solid samples (SPM and sediment) were used to determine the total organic carbon (TOC) contents by a total organic analyzer (TOC-LCPN, Shimadzu). For POP analysis, these solid samples (approximately 3 g) were spiked with the abovementioned surrogate standards, and extracted with mixed solvents (1:1 DCM and acetone for PAHs, 1:1 hexane and acetone for PCBs/OCPs, respectively) by an accelerated solvent extractor (ASE350, Thermo Fisher) at 100 °C and 1500 psi. The cleanup procedures of ASE extracts were performed by using a rotary evaporator and a silica-alumina column, based on our previous study (Yang et al., 2019). Then, the collected eluent was further evaporated to 1 mL under high purity nitrogen. The 200 ng internal standards were added

to the finally prepared samples before the instrument analysis.

Sixteen priority PAHs set by the US Environmental Protection Agency (EPA) including naphthalene (Nap), acenaphthylene (Acy), acenaphthene (Ace), fluorine (Fl), phenanthrene (Phe), anthracene (Ant), fluoranthene (Flu), pyrene (Pyr), benz[*a*]anthracene (BaA), chrysene (Chr), benzo[*b*]fluoranthene (BbF), benzo[*k*]fluoranthene (BkF), benzo[*a*]pyrene (BaP), indeno[*1, 2,* 3-cd]pyrene (InP), dibenz[*a, h*]anthracene (DahA), benzo[*ghi*]perylene (BghiP) were analyzed by using a gas chromatograph-mass spectrometer (GC 7890B-MS 5977A, Agilent) equipped with a HP-5ms quartz capillary column (30 m × 0.25 mm × 0.25 μm). Eighteen congeners of PCBs (PCB28, PCB52, PCB77, PCB81, PCB101, PCB105, PCB114, PCB118, PCB123, PCB126, PCB138, PCB153, PCB156, PCB157, PCB167, PCB169, PCB180, and PCB189) and twenty congeners of OCPs (α-HCH, β-HCH, γ-HCH, δ-HCH, p,p'-DDT, p,p'-DDE, p,p'-DDD, heptachlor, heptachlor epoxide, dieldrin, aldrin, γ-chlordane, α-chlordane, endrin, endosulfan-I, endosulfan-II, endrin aldehyde, endosulfan sulfate, methoxychlor, and endrin ketone) were measured by using a gas chromatograph-electronic capture detector (GC 7890A-ECD, Agilent) equipped with a DB-5 quartz capillary column (30 m × 0.25 mm × 0.25 μm). The basic information including molecular formula and octanol-water partition coefficients (log$K_{ow}$) of these target congeners were listed in Table S1 (S means the Supporting Information here and thereafter). The oven temperature programs for all studied POPs were different and set as follows: for PAHs, holding at 55 °C for 2 min, heating to 280 °C at a rate of 20 °C/min, and then heating to 300 °C at a rate of 3 °C/min for 4 min; for PCBs, holding at 60 °C for 1 min, heating to 140 °C at a rate of 20 °C/min, and then heating to 280 °C at a rate of 12 °C/min holding for 4 min; for OCPs, holding at 60 °C for 2 min, firstly heating to 180 °C at a rate of 30 °C/min holding for 4 min, secondly heating to 200 °C at a rate of 20 °C/min holding for 8 min, thirdly heating to 250 °C at a rate of 20 °C/min holding for 5 min, and finally heating to 280 °C at a rate of 30 °C/min holding for 8 min, respectively. The injection volume was 1 μL in splitless mode. The ion source and quadrupole temperature in MS detector were 320 °C and 150 °C in the selective ion monitoring mode, respectively. The ECD detector was maintained at a temperature of 280 °C for PCBs and 300 °C for OCPs, respectively.

### 2.3. Quality assurance and quality control (QA/QC)

To ensure QA/QC, one method blank, one standard-spiked blank and matrix, and one random duplicated sample were analyzed in every batch of 15 samples. Only low concentrations of Nap, Acy, Ace, Flo, Phe, Ant, PCB28, PCB77, PCB81, PCB123, HCH, DDE, DDD, heptachlor, and endosulfan-I were detected in method blanks. The recoveries of surrogate standards in standard-spiked blanks were 62.0%–111% for terphenyl-$d_{14}$ in PAH analysis, 70.8%–115% for 2,4,5,6-Tetrachloro-m-xylene in PCB analysis, and 93.4%–125% for 2,4,5,6-Tetrachloro-m-xylene in OCP analysis. The average recoveries of PAHs, PCBs, and OCPs in standard-spiked matrixes had a range of 62.8%–111%, 68.8%–117%, and 86.8%–128%, respectively. All the duplicated samples had a precision of lower than 20%. If the concentrations of individual POPs were under the method detection limit (MDL), they will be calculated as 1/2 of MDL. The concentrations of individual POPs investigated in this study were corrected by the surrogate recoveries after deducting their method blank values.

### 2.4. Health risk assessment model

#### 2.4.1. Water

For POPs in dissolved water, EPA calculation methods through oral exposure were applied to evaluate their carcinogenic and non-carcinogenic human health risks, as shown in the following Equations (1) and (2):

$$R_i = \frac{1 - \exp(-D_i \times CSF_i)}{AG} \quad (1)$$

$$R_j = \frac{D_i \times 10^{-6}}{RfD_i \times AG} \quad (2)$$

$$D_j = \frac{C_i \times IR_w \times EF \times ED}{BW \times AT} \quad (3)$$

Where $R_i$ and $R_j$ represent the average annual individual carcinogenic and non-carcinogenic risk of compound *i* caused by drinking water (1/a), respectively; $D_i$ is the daily average exposure dose per body weight (mg/kg/d); $CSF_i$ is the chronic oral slope factor of compound *i*, and $RfD_i$ is the reference dose of non-carcinogenic compound *i*, both acquired from USEPA's Integrated Risk Information System (IRIS, https://cfpub.epa.gov/ncea/iris_drafts/simple_list.cfm); $C_i$ is the average concentration of compound *i* in water samples from lake body (mg/L); *AG* is the average life expectancy in Shanghai, taking 83.37 a in 2017 according to Shanghai Health and Family Planning Commission (http://www.wsjsw.gov.cn/xwfb/20180525/31027.html); *EF* is the exposure frequency (365 d/a); *ED* is the exposure duration (83.37 a); $IR_w$ is the average adult daily water intake (2.2 L/d), and *BW* is the Chinese average body weight (62 kg), both obtained from Word Health Statistics (https://www.who.int/gho/publications/world_health_statistics/2015/en/); *AT* is the average time for carcinogenic and non-carcinogenic effect (30430.05 d).

#### 2.4.2. Fish

For POPs in fish, the carcinogenic risk (CR) through oral intake was calculated as the following Equation (4). The hazard quotient (HQ) was used to describe the non-carcinogenic risk, as shown in Equation (5).

$$CR = \frac{C_{ij} \times IR_f \times 10^{-3} \times CSF_i \times EF \times ED}{BW \times AT} \quad (4)$$

$$HQ = \frac{C_{ij} \times IR_f \times 10^{-3} \times EF \times ED}{RfD_i \times BW \times AT} \quad (5)$$

Where *Cij* denotes the average concentration of compound *i* in all fish samples (mg/g); $IR_f$ is the average adult daily consumption of freshwater fish in Shanghai (21.78 g/d), provided by Wu et al. (2013); Other parameters (*EF*, *ED*, *BW*, *AT*, *CSF*, and *RfD*) have the same meanings as those in section 2.4.1.

## 3. Results and discussion

### 3.1. Occurrence and distribution of POPs in water, SPM, and sediment

The annual average concentrations and standard errors of total PAHs ($\Sigma_{16}$PAHs), total PCBs ($\Sigma_{18}$PCBs), and total OCPs ($\Sigma_{20}$OCPs) in dissolved water, SPM, and surface sediment at all sampling sites (n = 11) were depicted in Fig. 2. By comparison, $\Sigma_{20}$OCPs had the highest concentrations in water dissolved phase with a range of 47.8–143 ng/L, while $\Sigma_{16}$PAHs had the highest concentrations in SPM and sediment phase with a range of 2805–4130 and 206–4262 ng/g, respectively (Fig. 2). Moreover, the mean concentrations of $\Sigma_{16}$PAHs (3416 and 1123 ng/g) in SPM and sediment phase, were 2–3 times greater than the average concentrations of $\Sigma_{18}$PCBs and $\Sigma_{20}$OCPs, suggesting that PAHs were the dominant compounds in SPM and sediment at all sites. Some studies have identified that the three groups of SPOPs would more tend to adsorb on the solid phase (SPM and sediment) in an aquatic ecosystem (Li et al., 2017; Liu et al., 2017). In this study, PAHs and PCBs mainly adsorbed on SPM compared to sediment, while OCPs were more found in sediment (Fig. 2). However, sediment resuspension caused by bioturbation and hydrodynamic change easily led to secondary pollution of SPM (Liu et al., 2017). Compared to those values reported in other drinking water sources of China (Li et al., 2017), the mean concentrations of $\Sigma_{16}$PAHs, $\Sigma_{18}$PCBs and $\Sigma_{20}$OCPs in

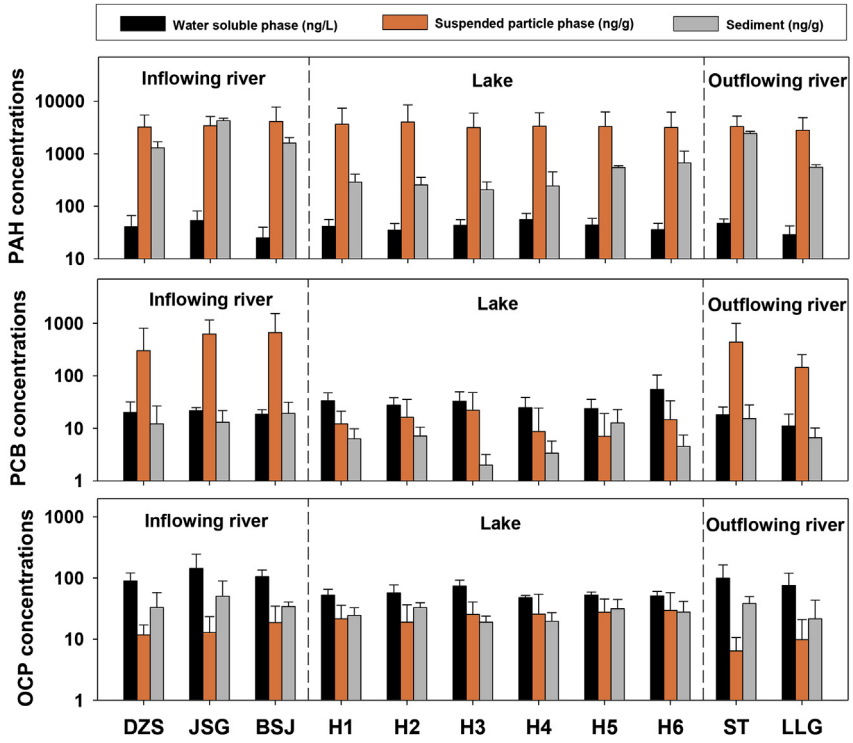


**Fig. 2.** Spatial distribution of annual average concentrations of $\Sigma_{16}$PAHs, $\Sigma_{18}$PCBs, and $\Sigma_{20}$OCPs in dissolved water, SPM, and surface sediment phases in Dianshan Lake watershed (the vertical bar represents standard error).

sediment phase (369, 6.01, and 25.8 ng/g, respectively) in lake body sites of DSL were lower than those in Lake Chaohu and Lake Taihu likewise located at the Yangtze River Delta Economic Zone of China, but far higher than such remote lakes as Lake Hulun, Lake Wulungu, Lake Basum, and Lake Namtso located in Mongolia Xinjiang Plateau and Qinghai Tibet Plateau of China.

As illustrated in Fig. 2, the annual average concentrations of $\Sigma_{16}$PAHs, $\Sigma_{18}$PCBs, and $\Sigma_{20}$OCPs in dissolved water, SPM, and sediment phase showed different spatial distribution. By means of the nonparametric test in SPSS 17.0, $\Sigma_{16}$PAH concentrations in dissolved water and SPM phase did not show significant differences among inflowing rivers, lake body, and outflowing rivers ($p > 0.05$), but the significantly lower concentrations were found in the lake sediment phase compared to inflowing/outflowing rivers ($p < 0.05$). No significant differences were found in $\Sigma_{18}$PCB and $\Sigma_{20}$OCP concentrations in sediment phase at all sites ($p > 0.05$), and in dissolved water and SPM phase between inflowing rivers with outflowing rivers ($p > 0.05$). However, $\Sigma_{18}$PCB concentrations in SPM phase and $\Sigma_{20}$OCP concentrations in dissolved water phase were significantly lower in lake body sites than inflowing rivers ($p < 0.05$). In general, the significantly higher concentrations of $\Sigma_{16}$PAHs in sediment, $\Sigma_{18}$PCBs in SPM, and $\Sigma_{20}$OCPs in dissolved water from inflowing rivers than lake body sites indicated the strong effect of riverine pollution input. Moreover, the significantly higher concentrations of $\Sigma_{18}$PCBs in dissolved water and $\Sigma_{20}$OCPs in SPM in lake body sites than inflowing and outflowing rivers ($p < 0.05$) suggested that DSL was their important reservoir in despite of water transportation toward downstream rivers.

The seasonal distributions of POPs in water, SPM, and sediment phase were illustrated in Fig. S1. The mean concentrations of $\Sigma_{16}$PAHs in SPM phase from both inflowing/outflowing rivers and lake body sites followed descending orders of winter > spring > autumn > summer. For $\Sigma_{16}$PAH concentrations in SPM phase, there were significantly seasonal disparities between winter with summer for inflowing rivers and lake body ($p < 0.05$). One probable explanation was attributed to the greater combustion emission of PAHs from coal and biomass energy in winter than summer. Another reason was that the PAHs photodegradation caused by the higher temperature and stronger sunshine in summer decreased adsorption capacity of PAHs on SPM phase (Goguo et al., 1996). The higher primary productivity and chlorophyll a abundance in summer in aquatic environment could also increase vertical migration of POPs on SPMs toward sediments, thus causing decreasing $\Sigma_{16}$PAH concentrations on summery SPMs compared to winter (Wong et al., 1995; Buesseler, 1998). The average concentrations of $\Sigma_{18}$PCBs in SPM phase had significantly lower values in summer than winter in inflowing and outflowing rivers, but just the opposite for lake body sites ($p < 0.05$). Likewise, $\Sigma_{20}$OCP concentrations in SPM phase in outflowing rivers and lake body were also observed similar characteristics with those of $\Sigma_{18}$PCBs. PCBs and OCPs in China have been forbidden since the 1980s (Wei et al., 2007), and their detections in lake ecosystem could be mainly due to the release of historical legacy from their early usage in surrounding areas. The frequent rainfall events in summer triggered stronger runoff erosion of bare soil and carried more particle matters into lake body. In this study, the higher concentration of SPMs in lake body exactly had been verified in summer (23.8 mg/L) than winter (20.9 mg/L). Moreover, the slower water velocity in lake body than surrounding rivers caused longer retention of SPMs and consequently more adsorption of pollutants. This could be an explanation for the higher concentrations of $\Sigma_{18}$PCBs and $\Sigma_{20}$OCPs in SPM phase from lake body in summer than winter. As depicted in Fig. S1, the higher concentrations of $\Sigma_{18}$PCBs and $\Sigma_{20}$OCPs in SPM phase from surrounding rivers of DSL in winter than summer were probably because the smaller river water volume in winter decreased the dilution effect on water-carrying pollutants. Fig. S1 showed that there were significantly greater $\Sigma_{20}$OCP concentrations in dissolved water from outflowing rivers in summer than winter ($p < 0.05$), mainly impacted by increasing agricultural activities in summer in adjacent areas. Although OCPs in China have been forbidden since the 1980s, their alternative products (e.g., lindane and dicofol) still contained some components of OCPs and were applied in agriculture production for pest control (Wei et al., 2007). Therefore, their

increasing agricultural application in summer and more enrichment tendency toward dissolved water phase could well explain why the $\Sigma_{20}$OCP concentrations in dissolved water from outflowing rivers were greater in summer than winter. For sediment phase, only $\Sigma_{18}$PCBs in inflowing and outflowing rivers had significantly lower concentrations in summer than other seasons ($p < 0.05$). This might be attributed to the strong scouring effect of river water in summer on bottom sediments caused by large water volume and high water velocity (Zhang and Zhang, 1992).

### 3.2. POP compositions and source indication

Homologue compositions of PAHs, PCBs, and OCPs presented obvious variations in different environmental media (i.e., water, SPM and sediment) of DSL and inflowing/outflowing rivers (Fig. 4). Their isomer profiles could be used as valuable indicators for their sources, transportation, and fate (Li et al., 2017).

For PAHs, low molecular weight (LMW, 2–3 ring) PAHs were the dominant homologues in water phase of all sampling sites (Fig. 4), averagely accounting for 63.9% of $\Sigma_{16}$PAHs. Some studies also found that LMW PAHs tend to dissolve in water phase due to their relative higher solubility than high molecular weight (HMW, 4–6 ring) PAHs (Hawthorne et al., 2005; Qin et al., 2014). However, HMW PAHs dominated in SPM and sediment phase of all sampling sites (Fig. 4), accounting for 52.3%–66.7% (average: 58.7%) and 81.2%–87.7% (average: 84.4%) of $\Sigma_{16}$PAHs, respectively. The high proportions of HMW PAHs in solid phases were closely attributed to their strong sorption capacity (Qin et al., 2014). Furthermore, the isomer ratios of PAHs such as Ant/(Ant + Phe), BaA/(BaA + Chr), Flu/(Flu + Pyr), and InP/(InP + BghiP) were applied to trace the possible sources of PAHs in the three phases. According to the source identification suggested by Yunker et al. (2002), the ratios of Ant/(Ant + Phe) were > 0.1 and the ratios of BaA/(BaA + Chr) were > 0.35 in the three phases (Fig. S2), indicating that 3- and 4-ring PAHs could be mainly derived from pyrogenic sources. The ratios of Flu/(Flu + Pyr) were > 0.5 in all phases (Fig. S2), corresponding to the combustion sources of grass, wood, and coal (Yunker et al., 2002). The ratios of InP/(InP + BghiP) varied from 0.2 to 1.0, also indicating complicated pyrogenic sources including liquid fossil combustion and gross, wood, and coal combustion (Fig. S2).

In China, about 10000 tons of PCBs mainly including trichlorobiphenyl (#1 PCB) and pentachlorobiphenyl (#2 PCB) were produced from 1965 to 1974 until manufacturing of commercial PCBs were banned (Ren et al., 2007). PCBs were widely used in power capacitors, insulation oils, lubricants in industry, and major additive of varnish, dielectric and plasticizers (Ren et al., 2007; Wang et al., 2018). According to the estimation by Ren et al. (2007), the chlorine proportions of #1 PCB and #2 PCB were similar to the imported products - Aroclor 1242 dominated by tri- and tetra-PCBs and Aroclor 1254 dominated by penta- and hexa-PCBs, respectively. Therefore, according to the different product usage and similar Aroclor profiles, the dominant congeners of PCBs had been widely acted as reliable source indicators (Li et al., 2017; Wang et al., 2018). The homologue compositions of PCBs in water, SPM, and sediment phase of DSL and inflowing/outflowing rivers were also illustrated in Fig. 4. In this study, tri-PCBs only detected PCB 28, and thus contributed very low proportion to $\Sigma_{18}$PCBs (Fig. 4). Overall, tetra-PCBs and penta-PCBs were the most dominant congeners in the water and SPM phase, with similar mean proportions for tetra-PCBs (23.7% and 26.0%, respectively) and penta-PCBs (39.3% and 39.4%, respectively). In China, tetra-PCBs were used as a major component in capacitor equipment, and penta-PCBs were used as additives in industrial products such as paint, carbonless copy paper, and cable insulation (Ren et al., 2007). These indicated that PCBs in water and SPM phase of DSL could mainly derived from the leakage of capacitor equipment, sewage drainage of industrial production, and exfoliation of ship paints. As shown in Fig. 4, hexa-PCBs contributed the maximum proportion to $\Sigma_{18}$PCBs in the sediment phase, with a range from 20.0% to 53.8% (average: 41.7%), followed by penta-PCBs (average: 27.1%) and tetra-PCBs (average: 25.4%). This also verified a fact that the highly chlorinated congeners with higher log$K_{ow}$ could be more likely to adsorb on sediment phase. Considering that hexa-PCBs were mainly from imported electrical capacitors (Huo et al., 2017), it was inferred that highly chlorinated (hexa- and penta-) PCB contaminations in sediment phase of DSL mainly derived from the leakage of imported electrical capacitors and various industrial activities. Similarly, high proportions of highly-chlorinated PCBs were also found in sediments located in close proximity to industrial discharges and urban runoff (Huo et al., 2017).

In this study, ΣHCHs (sum of α-HCH, β-HCH, γ-HCH, and δ-HCH) and ΣDDTs (sum of p,p'-DDT, p,p'-DDD, and p,p'-DDE) were the most dominant congeners among the 20 individual OCPs in the water, SPM, and sediment phase of DSL and inflowing/outflowing rivers, with a mean proportion of 22.6%–41.5% and 12.2%–39.0%, respectively (Fig. 4). Especially in sediment phase, HCHs and DDTs accounted for > 80% of $\Sigma_{20}$OCPs, reflecting their wide use in study region. Two types of HCH products were manufactured in China, of which 4.46 million tons of technical HCH (containing 65–70% α-HCH, 5–6% β-HCH, 12–14% γ-HCH, and 6% δ-HCH) were applied in 101 million ha of arable land from 1952 to 1983 (when technical HCH was banned in China), and another alternative product - lindane (consisting of > 99% γ-HCH) began to be used for pest control since 1991 (Li et al., 1998). Therefore, some researchers traced environmental sources of HCH based on a fact that the relatively stable ratio of α-/γ-HCH (4.64–5.83 for technical HCH and nearly 0 for lindane) might increase when α- and γ-HCH were degraded into β-HCH (Jiang et al., 2009). Their high ratio (α-/γ-HCH > 5.83) indicates the historical usage of technical HCH, and a low ratio means recent input of lindane. As shown in Table S2, the ranges of α-/γ-HCH ratio in the water, SPM and sediment phase of DSL and inflowing/outflowing rivers were 1.72–8.66, 0.56–9.14, and 0.08–19.0, respectively, suggesting the mixture input of technical HCH and lindane. The higher ratios of α-/γ-HCH were mainly found in the water phase of inflowing/outflowing rivers and in the SPM phase of outflowing rivers, indicating that rainfall runoff scour carried historical residue of technical HCH in agricultural soils into surrounding rivers. The low ratios of α-/γ-HCH in the water, SPM phase, and 50% sediment phase of lake body revealed the recent application of lindane in DSL area.

According to the statistics, over 430 kt of commercial DDT from 1951 to 1983 were produced mainly for agriculture application, but a small quantity of DDTs were still used for stock of dicofol, disease vector control, and producing mosquito-repellent incense and special paint after its agricultural use was banned in 1983 (Wei et al., 2007). Generally, p,p'-DDT could be degraded into p,p'-DDD and p,p'-DDE by microbe under anaerobic or aerobiotic condition (Liu et al., 2017). The ratios of p,p'-DDD/p,p'-DDE were < 1 in 72.7% water samples, 81.8% SPM samples, and 90.9% sediment samples, implying that p,p'-DDT was mainly aerobically degraded into DDE. The ratios between the parent compound and its two metabolites also provide valuable source indication (Jiang et al., 2009). As shown in Table S2, the ratio of p,p'-DDT/(p,p'-DDD + p,p'-DDE) in this study varied from 0.67 to 4.03 in water phase, from 0.31 to 3.11 in SPM phase, and from 0.42 to 17.2 in sediment phase of DSL and its surrounding rivers, suggesting DDT residues in the study region from historical and recent application. Especially, the recent input of DDT played key contribution because the ratios of p,p'-DDT/(p,p'-DDD + p,p'-DDE) were > 1 in 72.7% water samples and 91.8% sediment samples from DSL and its surrounding rivers.

### 3.3. POP bioaccumulations in fish

For the three groups of POPs, the ranges of their detection frequencies in the six fish species of DSL were 47.2%–100% for 16

individual PAHs, 25.0%–100% for 18 individual PCBs, 40.5%–100% for 20 individual OCPs, with an average of 92.1%, 62.1%, and 80.2%, respectively. Similar to their trends in sediment phase, the mean concentration of POPs in the six fish species also showed a descending order: $\Sigma_{16}$PAHs (353 ± 106 ng/g dw) > $\Sigma_{20}$OCPs (67.4 ± 27.0 ng/g dw) > $\Sigma_{18}$PCBs (32.0 ± 13.7 ng/g dw) (Table S3). Compared to archive data recorded in other studies in domestic and overseas (Wang et al., 2012) and in Table S4, the mean concentrations of $\Sigma_{18}$PCBs and $\Sigma_{20}$OCPs in fish species of DSL were at a low pollution level, but for $\Sigma_{16}$PAHs it was worthy to pay more attention due to its moderate pollution level.

In the six fish species, the highest concentration of $\Sigma_{16}$PAHs (596 ng/g dw) was detected in *Chanodichthys erythropterus*, followed by *Erythroculter ilishaeformis* (Table S3). In this study, the higher $\Sigma_{16}$PAH concentrations were found in carnivorous fish species at high trophic level, implying the impact of trophic level on PAH bioaccumulations in fish. Lipid contents of fish species change with species, age, water body environment and feeding habits. Generally, the higher lipid contents were measured in the fish species at high trophic level, which could lead to higher PAH bioaccumulations (Bandowe et al., 2014). Relationships between lipid content (not detected in this study) with PAH bioaccumulations need a further detailed study. As shown in Table S3, the most abundant compound of PAHs in the six fish species was 3-ring PAHs with a mean value of 200 ng/g dw, accounting for 56.7% of $\Sigma_{16}$PAHs. Generally, LMW (2–3 ring) PAHs with low log$K_{ow}$ values have the higher water solubility, higher bioavailability, and higher uptake rate compared to HMW (4–6 ring) PAHs with the higher depuration rate in fish due to the effect of enzymatic metabolism and low gut assimilation (Bandowe et al., 2014; Baumard et al., 1998). It has been reported that the bioaccumulations of PAHs in fish tissue are negatively correlated with log$K_{ow}$ values (Bandowe et al., 2014; Logan, 2007), thereby suggesting that equilibrium partitioning from water/sediment into fish tissue was the main mechanism of bioaccumulation. In addition, the feeding habits of carnivorous fish species can contribute for the higher bioaccumulation of LMW PAHs. Li et al. (2014) found that algaes and zooplanktons preferred to accumulate LMW PAHs along with increasing water eutrophication, thus impacting PAH bioaccumulations in fish species at low trophic level feeding on algaes and zooplanktons. Therefore, along with gradually increasing aggravation of water eutrophication in DSL (Zhang and Wang, 2009), LMW PAHs dominated in fish samples under the common effect of bioaccumulation in food chain and abovementioned partitioning equilibrium.

As shown in Table S3, the concentrations of $\Sigma_{18}$PCBs in the six fish species varied from 12.6 to 75.1 ng/g dw, but did not display obvious species-specific distribution characteristic due to the insignificant difference of mean $\Sigma_{18}$PCB concentrations among these fish species ($p < 0.05$). In this study, Σpenta-PCBs, Σtetra-PCBs and Σhexa-PCBs were dominant compounds in the six fish species, and their mean values in all the fish samples accounted for 41.6%, 26.4% and 22.1% of total concentrations, respectively. The distribution pattern of PCB congeners in fish samples of DSL was consistent with those in the water, SPM and sediment phase. This also indicated that the main routes of PCB bioaccumulations in fish were both from water by membrane diffusion and from contaminated sediments by dietary uptake.

In Table S3, the concentrations of $\Sigma_{20}$OCPs in the six fish species ranged from 29.1 to 142 ng/g dw with obviously variable mean values, indicating species-specific distribution characteristic. Consistent with $\Sigma_{18}$PCBs, the maximum concentration of $\Sigma_{20}$OCPs was also detected in *Pelteobagrus fulvidraco* (Table S3). The *Pelteobagrus fulvidraco* is a slower growth omnivorous fish, mainly feeds on creophagism, these characteristics causing higher accumulations of PCBs and OCPs. The most abundant compounds of OCPs in all fish species were ΣDDTs and ΣHCHs, with mean values accounting for 37.4% and 28.5% of total concentration, respectively. Low lipophilicity and high biodegradation caused a lower accumulation of HCHs in fish samples compared to its DDTs counterpart (Fu et al., 2018). The bioaccumulation of DDTs in fish was partly controlled by lipid content and biomagnification through food chain (Fu et al., 2018; Zhao et al., 2014).

In general, the bioaccumulations of POPs in different fish species were comprehensively impacted by their physiological and ecological features (e.g., feeding and life habits, trophic level, lipid content, and metabolic capacity) (Bandowe et al., 2014).

### 3.4. Partition of POPs in water-SPM-sediment-fish system

Some researches have verified that TOC content can influence the partition behavior and final fate of POPs in aquatic ecosystem (Li et al., 2017; Zhang et al., 2018). However, no significant relationships were found between the concentrations of $\Sigma_{16}$PAHs, $\Sigma_{18}$PCBs, and $\Sigma_{20}$OCPs with TOC contents (1.18%–6.65%) in the solid (SPM and sediment) samples of DSL ($p > 0.05$), probably impacted by the less sampling sites (n = 11). Therefore, the partition coefficients ($K_p$ and $K_s$) of three groups of POPs in the SPM - water system and sediment - water system of DSL were calculated respectively without TOC-normalized concentration correction, as Equations (6) and (7). Their bioconcentration factor (BCF) and bio-sediment accumulation factor (BSAF) in the DSL were also calculated respectively as Equations (8) and (9):

$$K_p = \frac{C_{SPM}}{C_{water}} \tag{6}$$

$$K_s = \frac{C_{Sediment}}{C_{water}} \tag{7}$$

$$BCF = \frac{C_{biota}}{C_{water}} \tag{8}$$

$$BSAF = \frac{C_{biota}}{C_{sediment}} \tag{9}$$

Where $C_{SPM}$, $C_{water}$, and $C_{sediment}$ represent the annual average concentrations of POPs in SPM phase (ng/g), water phase (ng/L), and sediment phase (ng/g) of DSL, respectively; $C_{biota}$ represents the average concentration (ng/g) of POPs in all fish samples collected from DSL.

As shown in Table S5, the partition coefficients ($K_p$ and $K_s$) of $\Sigma_{16}$PAH concentrations in solid phase (SPM and sediment) and dissolved water phase of DSL were significantly greater than those values of $\Sigma_{18}$PCBs and $\Sigma_{20}$OCPs ($p < 0.05$). This implied the stronger absorption capacity of PAHs on solid phases compared to PCBs and OCPs. The $K_p/K_s$ ratios of $\Sigma_{16}$PAHs, $\Sigma_{18}$PCBs, and $\Sigma_{20}$OCPs were above 1 (Table S5), indicating that they more tended to adsorb on SPM compared to sediment. However, for a few of PCB congeners (PCB156 and PCB169) and OCP congeners (α-HCH, β-HCH, γ-HCH, p,p'-DDT, p,p'-DDD, p,p'-DDE, heptachlor epoxide, and endosulfan sulfate), their $K_p$ values were lower than the $K_s$ values (Table S5), implying that these POPs more easily concentrated in sediment compared to SPM. Spearman correlation analysis further revealed significant relationships between log$K_{ow}$ with partition coefficients (log$K_p$ and log$K_s$) for PAH congeners ($p < 0.05$), and between log$K_{ow}$ with log$K_s$ for OCP congeners ($p < 0.05$). The regression coefficients ($R^2$) between log$K_p$, log$K_s$ and log$K_{ow}$ values were 0.503 and 0.751 (Fig. 3), respectively, indicating the hydrophobicity had a key influence on the partition behaviors of PAHs in the multiphase system of DSL. For PCB congeners, no significant relationships ($p > 0.05$) were found probably due to the lack of their log$K_{ow}$ values (Table S1). However, the increasing trends between their partition coefficients (log$K_p$ and log$K_s$) with log$K_{ow}$ values were still obvious in Fig. 3. For OCP congeners, the increasing trend between log$K_s$ with log$K_{ow}$ values implied that hydrophobic OCPs more tended to adsorb on sediment phase (Fig. 3). In addition, the higher SPM content can reduce log$K_p$ value, which influence the partitioning behavior of PAHs in the water-SPM system (Voice et al., 1983; Zhou et al., 1999). In this study, the seasonal variations of SPM content in the DSL were 20.85–30.27 mg/L, and had clear inverse correlation with the log$K_p$ values of PAHs ($p < 0.05$). Moreover, the significantly

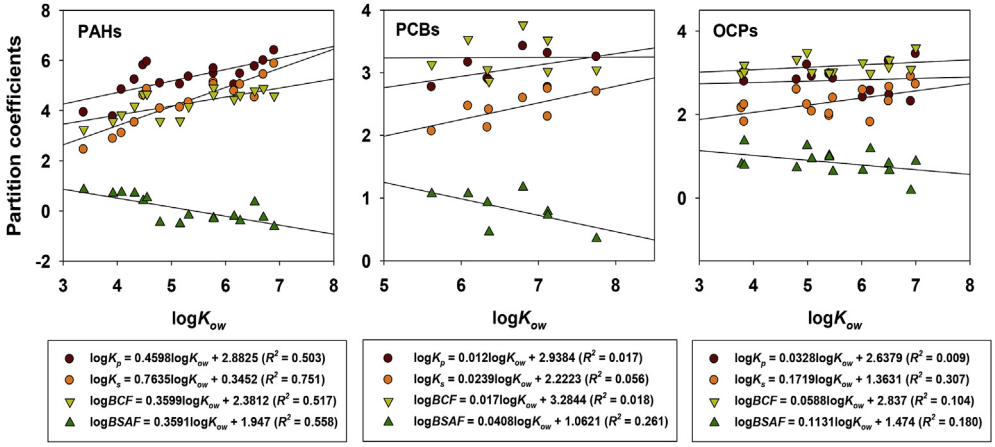


**Fig. 3.** Linear regression of individual log$K_{ow}$ of PAHs, PCBs, and OCPs and their partition coefficients (log$K_p$, log$K_s$, log*BCF*, and log*BSAF*) in the multiphase system of Dianshan Lake.

lower SPM content in the DSL than urban river net of Shanghai (50–218.8 mg/L, Wang et al., 2017) also explained the greater $K_p$ value of $\Sigma_{16}$PAHs in the DSL ($7.50 \times 10^6$ L/kg) than the latter ($1.77 \times 10^4$–$5.28 \times 10^5$ L/kg, Liu et al., 2016).

In this study, the BCF values of all congeners of POPs varied from $2.48 \times 10^2$ L/kg to $8.17 \times 10^4$ L/kg (Table S5), implying that POP concentrations in fishes far exceeded than those in water and these POPs had a high bioaccumulation in fish samples. As shown in Table S5, the mean BCF values of these POP congeners had a decreasing order: PAH congeners ($3.21 \times 10^4$ L/kg) > PCB congeners ($2.66 \times 10^3$ L/kg) > OCP congeners ($1.46 \times 10^3$ L/kg). This indicated that the fish species vigorously exchange PAHs through gills compared to PCBs and

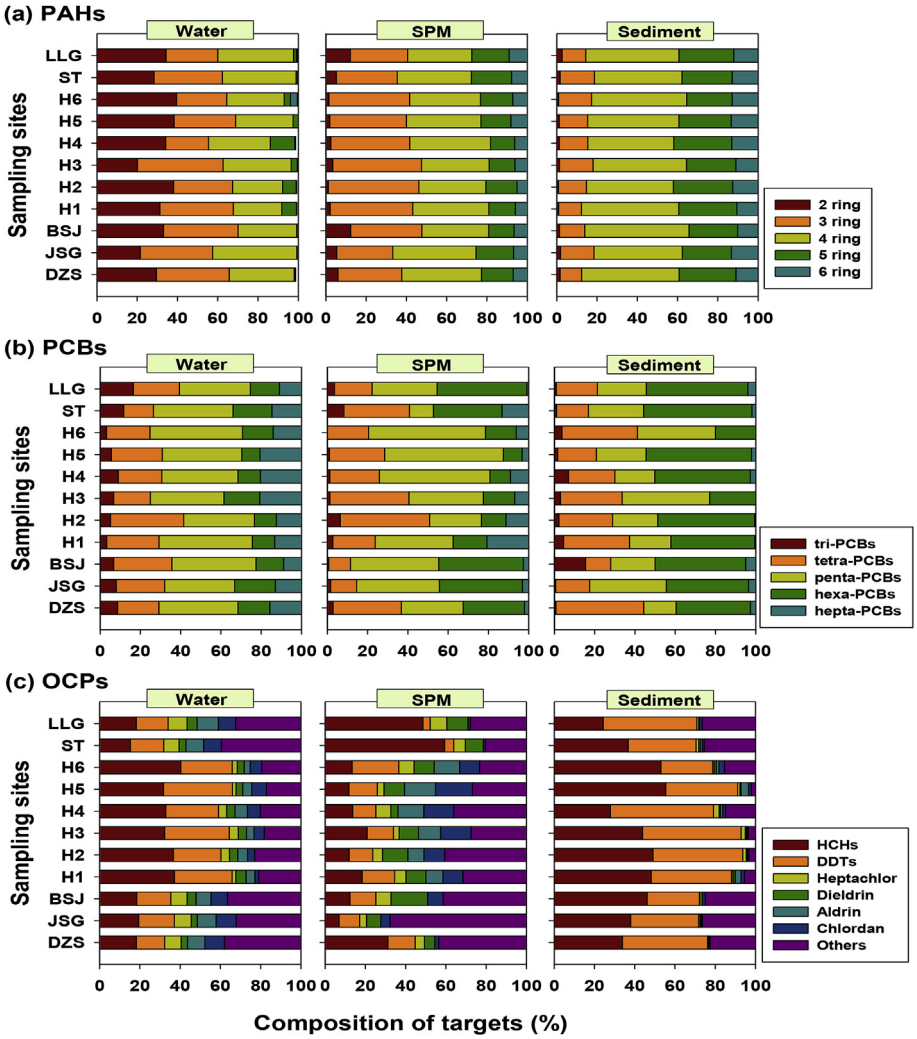


**Fig. 4.** Relative abundances of homologue compositions of PAHs, PCBs, and OCPs in dissolved water, SPM, and surface sediment phases in Dianshan Lake watershed.

**Table 1**
Human health risks of POPs in dissolved water and fish samples from Dianshan Lake through oral exposure.

| Compound | Noncarcinogenic parameter | Carcinogenic parameter | Concentration | | Water | | Fish | |
|---|---|---|---|---|---|---|---|---|
| | RfD (mg/kg/d) | CSF (kg·d/mg) | Water (mg/L) | Fish (mg/g) | Non-carcinogenic risk (1/a) | Carcinogenic risk (1/a) | Non-carcinogenic risk | Carcinogenic risk |
| **PAHs** | | | | | **1.53E-08** | **2.36E-06** | **1.97E-05** | **8.34E-08** |
| Nap | 2.00E-02 | NA | 1.51E-05 | 2.67E-05 | 9.06E-12 | – | 4.70E-07 | – |
| Acy | NA | NA | 2.38E-06 | 1.63E-05 | – | – | – | – |
| Ace | 6.00E-02 | NA | 5.02E-06 | 1.86E-05 | 1.00E-12 | – | 1.09E-07 | – |
| Fl | 3.00E-02 | NA | 1.84E-06 | 2.81E-05 | 7.37E-13 | – | 3.29E-07 | – |
| Phe | NA | NA | 1.48E-06 | 6.68E-05 | – | – | – | – |
| Ant | 3.00E-01 | NA | 1.60E-06 | 7.38E-05 | 6.38E-14 | – | 8.64E-08 | – |
| Flu | 4.00E-02 | NA | 5.42E-06 | 2.12E-05 | 1.62E-12 | – | 1.86E-07 | – |
| Pyr | 3.00E-02 | NA | 3.37E-06 | 1.27E-05 | 1.35E-12 | – | 1.49E-07 | – |
| BghiP | NA | NA | 1.45E-07 | 5.62E-06 | – | – | – | – |
| Chr | NA | 7.30E-03 | 2.32E-04 | 1.90E-05 | – | 7.21E-10 | – | 4.86E-11 |
| BaA | NA | 7.30E-01 | 1.32E-03 | 1.92E-05 | – | 4.09E-07 | – | 4.93E-09 |
| BbF | NA | 7.30E-01 | 3.13E-04 | 1.36E-05 | – | 9.74E-08 | – | 3.50E-09 |
| BkF | NA | 7.30E-02 | 3.76E-04 | 1.06E-05 | – | 1.17E-08 | – | 2.72E-10 |
| BaP | 3.00E-04 | 7.30E+00 | 3.81E-04 | 1.57E-05 | 1.52E-08 | 1.18E-06 | 1.84E-05 | 4.02E-08 |
| DahA | NA | 7.30E+00 | 1.95E-04 | 1.22E-05 | – | 6.04E-07 | – | 3.14E-08 |
| InP | NA | 7.30E-01 | 1.56E-04 | 1.19E-05 | – | 4.83E-08 | – | 3.05E-09 |
| **PCBs** | 2.00E-05 | 2.00E+00 | 3.29E-05 | 3.20E-05 | **1.97E-08** | **2.80E-08** | **5.62E-04** | **2.25E-08** |
| **OCPs** | | | | | **1.62E-09** | **4.47E-08** | **4.63E-05** | **3.97E-08** |
| α-HCH | NA | 6.30E+00 | 6.03E-06 | 7.51E-06 | – | 1.62E-08 | – | 1.66E-08 |
| β-HCH | NA | 1.80E+00 | 6.78E-06 | 5.27E-06 | – | 5.20E-09 | – | 3.33E-09 |
| γ-HCH | 3.00E-04 | NA | 2.94E-06 | 3.76E-06 | 1.18E-10 | – | 4.40E-06 | – |
| δ-HCH | NA | NA | 4.40E-06 | 4.06E-06 | – | – | – | – |
| p,p'-DDD | NA | 2.40E-01 | 3.42E-06 | 5.97E-06 | – | 3.49E-10 | – | 5.03E-10 |
| p,p'-DDT | 5.00E-04 | 3.40E-01 | 8.50E-06 | 1.03E-05 | 2.04E-10 | 1.23E-09 | 7.27E-06 | 1.24E-09 |
| p,p'-DDE | NA | 3.40E-01 | 4.58E-06 | 9.29E-06 | – | 6.63E-10 | – | 1.11E-09 |
| Heptachlor | 5.00E-04 | 4.50E+00 | 1.84E-06 | 1.96E-06 | 4.40E-11 | 3.52E-09 | 1.37E-06 | 3.09E-09 |
| Heptachlor epoxide | 1.30E-05 | 9.10E+00 | 5.89E-07 | 3.99E-07 | 5.43E-10 | 2.28E-09 | 1.08E-05 | 1.28E-09 |
| total chlordan (α and γ) | 5.00E-04 | 3.50E-01 | 3.93E-06 | 6.94E-06 | 9.43E-11 | 5.85E-10 | 4.87E-06 | 8.53E-10 |
| total Endosulfan (I and II) | 6.00E-03 | NA | 4.81E-06 | 6.03E-06 | 9.61E-12 | – | 3.53E-07 | – |
| Dieldrin | 5.00E-05 | 1.60E+01 | 2.17E-06 | 2.08E-06 | 5.20E-10 | 1.48E-08 | 1.46E-05 | 1.17E-08 |
| Endrin | 3.00E-04 | NA | 2.26E-06 | 2.25E-06 | 9.05E-11 | – | 2.64E-06 | – |

The purple fonts means that these data were obtained from EPA's Integrated Risk Information System (IRIS, https://cfpub.epa.gov/ncea/iris_drafts/simple_list.cfm), and NA means not available in EPA's IRIS; the CSF values of carcinogenic PAHs in blue fonts were listed in USEPA (1998); the data in black bold means the total risk values of PAHs, PCBs, and OCPs calculated from the selected compounds.

OCPs. The mean BSAF values of PAH, PCB, and OCP congeners were 2.15, 19.2, and 6.83 (Table S5), suggesting that PAH congeners had the weakest bioaccumulation capacity via oral ingestion of contaminated sediments. According to a general rule provided by Landrum (1989), gills and skin play major role if POPs $\log K_{ow} < 5$, oppositely oral ingestion plays key role if POPs $\log K_{ow} > 5$. Fig. 3 revealed that only PAH congeners had significant relationships between their log*BCF*/log*BSAF* values with $\log K_{ow}$ values ($r^2 = 0.517/0.558$, $p < 0.05$). Therefore, we deduced that the equilibrium partitioning from water/sediment into fish muscle tissue was the main mechanism of PAH bioaccumulations, consistent with the research result obtained by Bandowe et al. (2014). For PAHs, the BSAF values of HMW PAHs (except DahA) were lower than 1 (Table S5). One explanation was because highly hydrophobic HMW PAHs with $\log K_{ow}$ greater than 5 might not be able to permeate fish membranes due to their large molecular dimensions (Gobas et al., 1988). Moreover, the enhanced biotransformation and decreased gut assimilation (dietary uptake) also resulted in low accumulation of highly hydrophobic PAHs in fishes (Bandowe et al., 2014; Liang et al., 2007). Inconsistent with PAHs, the BSAF values of all PCB congeners and OCP congeners (except heptachlor epoxide, endosulfan sulfate) were greater than 1 (Table S5), suggesting their strong bioaccumulation capacity from sediment. However, for PCBs and OCPs, no significant relationships were observed between their log*BSAF* values with $\log K_{ow}$ values ($p > 0.05$) (Fig. 3), indicating that the transfer route from the gut to the fish body via consuming sediments could play a predominant role compared to two-phase (from sediment to fish) partition. In addition, the highest BSAFs values of $\Sigma_{18}$PCBs (7.29) and $\Sigma_{20}$OCPs (4.40) were found in bottom-dwelling omnivorous fish species, such as *Pelteobagrus fulvidraco* This also suggested that the feeding habits (e.g., sediment-feeding behavior) of fish species can largely affect the bioaccumulations of PCBs and OCPs.

### 3.5. Health risk assessment of POPs in water and fish

Health risk assessments of POPs in dissolved water and fish samples of DSL through oral exposure were evaluated by EPA calculation models (Table 1). As shown in Table 1, the carcinogenic and non-carcinogenic risks of $\Sigma_{16}$PAHs and $\Sigma_{18}$PCBs, and carcinogenic risk of $\Sigma_{13}$OCPs in dissolved water varied from 1.97E-08 to 2.36E-06 1/a, which were higher than the negligible level (1.00E-08 1/a) proposed by the Dutch Ministry of Construction and the Environment. Especially, the carcinogenic risk of $\Sigma_{16}$PAHs (2.36E-06 1/a) was over two times higher than the maximum acceptable level (1.00E-06 1/a) recommended by the Swedish Environmental Protection Agency. The non-carcinogenic risks of total OCPs in dissolved water were underestimated probably due to the lack of non-carcinogenic parameter of other seven congeners. In general, the carcinogenic risks of all compounds were much higher than their non-carcinogenic risks. BaP and α-HCH were the key focus congeners with the highest carcinogenic risks for PAHs and OCPs, respectively. The carcinogenic risks resulting from lifetime exposure to $\Sigma_{16}$PAHs, $\Sigma_{18}$PCBs, and $\Sigma_{13}$OCPs via fish consumption were 8.34E-08, 2.25E-08, and 3.97E-08 (Table 1), far lower

than the acceptable guideline value of 1.00E-06 set by USEPA. These values indicated that only 225–834 persons per one billion population would be subjected to carcinogenic risk by eating fish food from DSL. The HQ values of $\Sigma_{16}$PAHs, $\Sigma_{18}$PCBs, and $\Sigma_{13}$OCPs caused by fish consumption were below one, ranging from 1.97E-05 to 5.62E-04, suggesting their non-carcinogenic risks were also very low but far greater than their carcinogenic risks. BaP and dieldrin had the highest non-carcinogenic risks for PAHs and OCPs, with a contribution rate of 93% and 32% to total risk level, respectively.

## 4. Conclusions

A systematic investigation of selected SPOPs including PAHs, PCBs, and OCPs was conducted in the water-SPM-sediment-fish system of DSL watershed, revealing prevalent SPOP contaminations and their different distribution characteristics. The significantly higher concentrations of $\Sigma_{16}$PAHs in sediment, $\Sigma_{18}$PCBs in SPM, and $\Sigma_{20}$OCPs in dissolved water from inflowing rivers than lake body suggested the strong effect of riverine pollution input. Their significant season variations were mainly attributed to the change of hydrodynamic conditions and source disparities. Source analysis further revealed that PAHs could mainly derive from pyrogenic sources related to fuel and biomass combustion, PCBs from the leakage of capacitor equipment, sewage drainage of industrial activities, and exfoliation of ship paints, HCH from the mixture input of technical HCH and lindane, and DDT from historical and recent application. Most of SPOPs in the six fish species of DSL showed obvious species-specific characteristic, comprehensively impacted by their physiological and ecological features. The partitioning behaviors of PAH congeners in the multiphase system of DSL were closely impacted by their log$K_{ow}$ values. However, sediment-feeding habits of fish species can largely affect the bioaccumulation of PCB and OCP congeners. The carcinogenic risks (below the acceptable guideline value) and HQ values (below one) resulting from lifetime exposure to $\Sigma_{16}$PAHs, $\Sigma_{18}$PCBs, and $\Sigma_{13}$OCPs via fish consumption implied a relative safety level at present. However, the carcinogenic risk of $\Sigma_{16}$PAHs in dissolved water should be noted due to being over two times higher than the maximum acceptable level.

## Acknowledgments

The authors express their appreciation for the financial support by the National Natural Science Foundation of China (No. 41601526 and 41730646), the China Scholarship Council.

## Appendix A. Supplementary data

Supplementary data to this article can be found online at https://doi.org/10.1016/j.apgeochem.2019.04.023.

## References

Bandowe, B.A.M., Bigalke, M., Boamah, L., Nyarko, E., Saalia, F.K., Wilcke, W., 2014. Polycyclic aromatic compounds (PAHs and oxygenated PAHs) and trace metals in fish species from Ghana (West Africa): bioaccumulation and health risk assessment. Environ. Int. 65, 135–146.

Baumard, P., Budzinski, H., Garrigues, P., Sorbe, J.C., Burgeot, T., Bellocq, J., 1998. Concentrations of PAHs in various marine organisms in relation to those in sediments and to trophic level. Mar. Pollut. Bull. 36, 951–960.

Bettinetti, R., Quadroni, S., Boggio, E., Galassi, S., 2016. Recent DDT and PCB contamination in the sediment and biota of the como bay (lake como, Italy). Sci. Total Environ. 542, 404–410.

Buesseler, K.O., 1998. The decoupling of production and particulate export in the surface ocean. Glob. Biogeochem. Cycles 12, 297–310.

Carlson, D.L., Swackhamer, D.L., 2006. Results from the US Great Lakes fish monitoring program and effects of lake processes on bioaccumulative contaminant concentrations. J. Gt. Lakes Res. 32, 370–385.

Fu, L., Lu, X.B., Tan, J., Zhang, H.J., Zhang, Y.C., Wang, S.Q., Chen, J.P., 2018. Bioaccumulation and human health risks of OCPs and PCBs in freshwater products of Northeast China. Environ. Pollut. 242, 1527–1534.

Gobas, F.A., Lahittete, J.M., Garofalo, G., Shiu, W.Y., Mackay, D., 1988. A novel method for measuring membrane-water partition coefficients of hydrophobic organic chemicals: comparison with 1-octanol-water partitioning. J. Pharm. Sci. 77, 265–272.

Goguo, A., Stratigakis, N., Kanakidou, M., Stephanou, E.G., 1996. Organic aerosols in Eastern Mediterranean: components source reconciliation by using molecular markers and atmospheric back trajectories. Org. Geochem. 5 (1), 79–96.

Hawthorne, S.B., Grabanski, C.B., Miller, D.J., Kreitinger, J.P., 2005. Solid-phase microextraction measurement of parent and alkyl polycyclic aromatic hydrocarbons in milliliter sediment pore water samples and determination of K DOC values. Environ. Sci. Technol. 39, 2795–2803.

Huo, S., Li, C., Xi, B., Yu, Z., Yeager, K.M., Wu, F., 2017. Historical record of polychlorinated biphenyls (PCBs) and special occurrence of PCB 209 in a shallow freshwater lake from eastern China. Chemosphere 184, 832–840.

Jiang, Y.F., Wang, X.T., Jia, Y., Wang, F., Wu, M.H., Sheng, G.Y., Fu, J.M., 2009. Occurrence, distribution and possible sources of organochlorine pesticides in agricultural soil of Shanghai, China. J. Hazard Mater. 170, 989–997.

Landrum, P.F., 1989. Bioavailability and toxicokinetics of polycyclic aromatic hydrocarbons sorbed to sediments for the amphipod Pontoporeia hoyi. Environ. Sci. Technol. 23, 588–595.

Li, C., Huo, S., Yu, Z., Xi, B., Yeager, K.M., He, Z., Ma, C., Zhang, J., Wu, F., 2017. National investigation of semi-volatile organic compounds (PAHs, OCPs, and PCBs) in lake sediments of China: occurrence, spatial variation and risk assessment. Sci. Total Environ. 579, 325–336.

Li, H., Lu, L., Huang, W., Yang, J., Ran, Y., 2014. In-situ partitioning and bioconcentration of polycyclic aromatic hydrocarbons among water, suspended particulate matter, and fish in the Dongjiang and Pearl Rivers and the Pearl River Estuary, China. Mar. Pollut. Bull. 83, 306–316.

Li, Y., Cai, D., Singh, A., 1998. Technical hexachlorocyclohexane use trends in China and their impact on the environment. Arch. Environ. Contam. Toxicol. 35, 688–697.

Liang, Y., Tse, M., Young, L., Wong, M., 2007. Distribution patterns of polycyclic aromatic hydrocarbons (PAHs) in the sediments and fish at Mai Po Marshes Nature Reserve, Hong Kong. Water Res. 41, 1303–1311.

Liu, C., Zhang, L., Fan, C., Xu, F., Chen, K., Gu, X., 2017. Temporal occurrence and sources of persistent organic pollutants in suspended particulate matter from the most heavily polluted river mouth of Lake Chaohu, China. Chemosphere 174, 39–45.

Liu, S., Liu, X., Liu, M., Yang, B., Cheng, L., Li, Y., Qadeer, A., 2016. Levels, sources and risk assessment of PAHs in multi-phases from urbanized river network system in Shanghai. Environ. Pollut. 219, 555–567.

Logan, D.T., 2007. Perspective on ecotoxicology of PAHs to fish. Hum. Ecol. Risk. Assess. 13, 302–316.

Qin, N., He, W., Kong, X.Z., Liu, W.X., He, Q.S., Yang, B., Wang, Q.M., Yang, C., Jiang, Y.J., Jorgensen, S.E., Xu, F.L., Zhao, X.L., 2014. Distribution, partitioning and sources of polycyclic aromatic hydrocarbons in the water–SPM–sediment system of Lake Chaohu, China. Sci. Total Environ. 496, 414–423.

Ren, N., Que, M., Li, Y.F., Liu, Y., Wan, X., Xu, D., Sverko, E., Ma, J., 2007. Polychlorinated biphenyls in Chinese surface soils. Environ. Sci. Technol. 41, 3871–3876.

USEPA, 1998. Guidelines for Ecological Risk Assessment. Washington, DC, USA. http://www.epa.gov/ncea/raf/pdfs/ecotxtbx.pdf.

Voice, T.C., Rice, C.P., Weber, W.J., 1983. Effect of solids concentration on the sorptive partitioning of hydrophobic pollutants in aquatic systems. Environ. Sci. Technol. 17, 513–518.

Wang, D.Q., Yu, Y.X., Zhang, X.Y., Zhang, S.H., Pang, Y.P., Zhang, X.L., Yu, Z.Q., Wu, M.H., Fu, J.M., 2012. Polycyclic aromatic hydrocarbons and organochlorine pesticides in fish from Taihu Lake: their levels, sources, and biomagnification. Ecotoxicol. Environ. Saf. 82, 63–70.

Wang, D., Wang, Y., Singh, V.P., Zhu, J., Jiang, L., Zeng, D., Liu, D., Zeng, X., Wu, J., Wang, L., 2018. Ecological and health risk assessment of PAHs, OCPs, and PCBs in Taihu Lake basin. Ecol. Indicat. 92, 171–180.

Wang, X., Han, J., Bi, C., Huang, X., Jia, J., Chen, Z., 2017. Distribution, sources, and risk assessment of polychlorinated biphenyls in surface waters and sediments of rivers in Shanghai, China. Front. Earth Sci. 11, 283–296.

Wei, D., Kameya, T., Urano, K., 2007. Environmental management of pesticidal POPs in China: past, present and future. Environ. Int. 33, 894–902.

Wong, C.S., Sanders, G., Engstrom, D.R., Long, D.T., Swackhamer, D.L., Eisenreich, S.J., 1995. Accumulation, inventory, and diagenesis of chlorinated hydrocarbons in Lake Ontario sediments. Environ. Sci. Technol. 35, 1567–1573.

Wu, C., Liu, H., Qin, L., Luo, B., Fang, Y., Yuan, W., Cai, H., 2013. Probability assessment of cadmium exposure level from aquatic food in Shanghai residents. J. Environ. Occup. Med. 2, 89–97.

Yang, J., Yang, Y., Liu, M., Meng, X.Z., Huang, Y.P., Zhang, X., Ma, F.Q., 2019. Comparing and modeling sedimentary profiles of elemental carbon and polycyclic aromatic hydrocarbons between early-and newly-urbanized areas in Shanghai. Environ. Pollut. 244, 971–979.

Yunker, M.B., Macdonald, R.W., Vingarzan, R., Mitchell, R.H., Goyette, D., Sylvestre, S., 2002. PAHs in the Fraser River basin: a critical appraisal of PAH ratios as indicators of PAH source and composition. Org. Geochem. 33, 489–515.

Zhang, J., Zhang, S., 1992. Preliminary study on water resources of Dianshan Lake. J. Lake Sci. 4, 009.

Zhang, X.H., Wang, Q., 2009. Evaluation of water quality and eutrophication in Dianshan Lake. The Administration and Technique of Environmental Monitoring 2, 024.

Zhang, X., Wang, T., Gao, L., Feng, M., Qin, L., Shi, J., Cheng, D., 2018. Polychlorinated diphenyl ethers (PCDEs) in surface sediments, suspended particulate matter (SPM) and surface water of Chaohu Lake, China. Environ. Pollut. 241, 441–450.

Zhao, Z.H., Wang, Y.Y., Zhang, L., Cai, Y.J., Chen, Y.W., 2014. Bioaccumulation and tissue distribution of organochlorine pesticides (OCPs) in freshwater fishes: a case study performed in Poyang Lake, China's largest lake. Environ. Sci. Pollut. Res. 21, 8740–8749.

Zhou, J., Fileman, T., Evans, S., Donkin, P., Readman, J., Mantoura, R., Rowland, S., 1999. The partition of fluoranthene and pyrene between suspended particles and dissolved phase in the Humber Estuary: a study of the controlling factors. Sci. Total Environ. 243, 305–321.